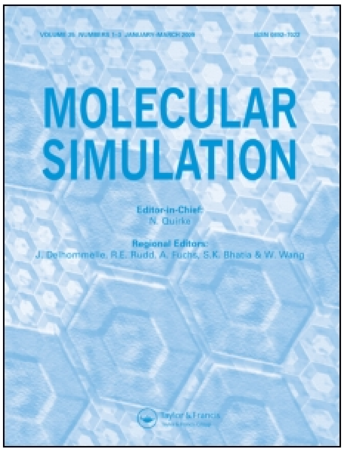

**Molecular Simulation**
Publication details, including instructions for authors and subscription information:
http://www.informaworld.com/smpp/title~content=t713644482

# Cage opening and fragmentation of $C_{60}$ fullerene induced by an ultrashort laser pulse

Hong Tang[a]; Hongjian Li[a]; Yusheng Dou[ab]; Weihai Fang[c]
[a] Institute of Computational Chemistry, Chongqing University of Posts and Telecommunications, Chongqing, P.R. China [b] Department of Physical Sciences, Nicholls State University, Thibodaux, LA, USA [c] Department of Chemistry, Beijing Normal University, Beijing, P.R. China

**To cite this Article** Tang, Hong , Li, Hongjian , Dou, Yusheng and Fang, Weihai(2010) 'Cage opening and fragmentation of $C_{60}$ fullerene induced by an ultrashort laser pulse', Molecular Simulation, 36: 12, 986 — 991
**To link to this Article: DOI:** 10.1080/08927022.2010.498827
**URL:** http://dx.doi.org/10.1080/08927022.2010.498827

*Molecular Simulation*
Vol. 36, No. 12, October 2010, 986–991

# Cage opening and fragmentation of $C_{60}$ fullerene induced by an ultrashort laser pulse

Hong Tang[a], Hongjian Li[a], Yusheng Dou[ab]* and Weihai Fang[c]

[a] *Institute of Computational Chemistry, Chongqing University of Posts and Telecommunications, Chongqing 400065, P.R. China;* [b] *Department of Physical Sciences, Nicholls State University, P.O. Box 2022, Thibodaux, LA 70310, USA;* [c] *Department of Chemistry, Beijing Normal University, Beijing 100875, P.R. China*

(*Received 4 February 2010; final version received 2 June 2010*)

Response of $C_{60}$ fullerene to a 40 fs full-width at half-maximum laser pulse with a photon energy of 2.0 eV and different laser intensities is studied by semiclassical dynamics simulation technique. The simulation results show that soon after the irradiation with a strong laser pulse, many C—C bonds abruptly break but no fragments are produced. The breaking of multiple C—C bonds induces a quick increase in the kinetic energy and potential energy and a decrease in electronic energy. These results suggest that the opening of the $C_{60}$ cage is an effective channel for the conversion of electronic energy to kinetic energy for the electronically excited $C_{60}$ fullerene.

**Keywords:** fullerene; semiclassical; dynamics simulation; ultrashort laser

## 1. Introduction

Fullerene ($C_{60}$) exhibits an extremely fast response upon laser irradiation [1–3], and therefore becomes a model system for studying the electronic and nuclear dynamics induced by ultrafast laser pulses [4,5].

One of the interesting topics in this field is photon fragmentation of $C_{60}$ [1–6]. Assisted with mass spectroscopy, the fragmentation patterns of $C_{60}$ have been quite well studied experimentally and theoretically [2,4–9]. However, the mechanism behind photo-induced fragmentation is not well understood. It has been suggested that the fragmentation at different laser pulse durations follows different mechanisms [7,10–12]. For nanosecond laser pulses, mass spectrum shows a bimodal mass distribution with a series of small fragments $C_n$ and large fragments $C_{60-2n}$ generated by a sequential loss of $C_2$ unit [2]. This fragmentation pattern can be explained by statistical processes since nanosecond excitation allows fullerene to achieve the complete equilibration of electronic energy and thermal energy through coupling between vibrational and electronic degrees of freedom [7]. For femtosecond laser pulses, the mass spectrum shows a large distribution of multiple-charged heavy fragments [3,4]. As the excitation time scale is smaller than or similar to the electron–phonon coupling time ($\sim$250 fs) [7], the response of $C_{60}$ fullerene to ultrafast excitation becomes more complicated [10–12]. It has been proposed that the relaxation of femtosecond laser excitations is proceeded through different channels, including thermal and non-thermal fragmentations, which produce a superposition of ionised and neutral fragments [3,12]. When the duration of a laser pulse is as short as 9 fs, which is well below the characteristic time scale for electron–phonon coupling, the excitation generates a fragmentation pattern which is predominated by $C_{60}^{+}$ ions at low laser intensities [3].

All experimental observations suggest that laser-induced fragmentation is a complicated process. Several mechanisms might be responsible for these observations [3]. $C_{60}$ has an icosahedral symmetry closed cage structure, which consists of 32 faces with 20 being hexagonal and 12 being pentagonal. In $C_{60}$, each carbon atom is bonded to three others through $sp^2$ hybridisation. Upon irradiation with a laser pulse, the cage of $C_{60}$ fullerene vibrates and the C—C bonds break. The breakage of any C—C bond leads to the opening of a $C_{60}$ cage and the fragments are released after the $C_{60}$ cage is opened. $C_{60}$ cage opening is therefore a primary event for fragmentation. Examination of this fundamental process can provide supplemental information for understanding fragmentation mechanisms. Mass spectroscopy cannot provide any information on cage opening, as mass spectrum displays the ratio of the mass of a $C_{60}$ over only its charge, but does not show the conformational feature of the $C_{60}$. In this paper, we report a semiclassical dynamics simulation study of the cage opening of an isolated $C_{60}$ fullerene irradiated by a 40 fs (full-width at half-maximum, FWHM) laser pulse. The simulation study is focused just on excitations below the continuum levels and the relaxation channels lead to the formation of neutral fragments. Although ionisation is an important channel of de-excitation especially at high laser intensity, Jeschke and co-workers [13] concluded from the phase-space argument that the processes without ionisation of the $C_{60}$ fullerene

---

*Corresponding author. Email: yusheng.dou@nicholls.edu

ISSN 0892-7022 print/ISSN 1029-0435 online

DOI: 10.1080/08927022.2010.498827
http://www.informaworld.com

should contribute significantly to the relaxation channels if the laser intensity is not extremely high.

## 2. Methodology

In the semiclassical dynamics simulation method, the state of the valence electrons is calculated by the time-dependent Schrödinger equation, but the radiation field and the motion of the nuclei are treated classically. A detailed description of this method has been published elsewhere [14,15], so only a very brief explanation is presented here. The total energy of a molecule is described by

$$E_{\text{total}} = \sum_{i}^{\text{occ}} \langle \Psi_i | H_0 | \Psi_i \rangle + \sum_{\alpha>\beta} U_{\text{rep}}(|X_\alpha - X_\beta|), \quad (1)$$

where the first term is electronic energy and the sum goes over occupied Kohn–Sham orbitals, which are presented by an optimised linear combination of atomic orbitals (LCAO) basis set. The second term is the effective repulsion potential, which is approximated as a sum of two-body potentials as follows:

$$E_{\text{rep}} = \sum_{\alpha>\beta} U_{\text{rep}}(|X_\alpha - X_\beta|). \quad (2)$$

The Hamiltonian matrix elements, overlap matrix elements and effective nuclear–nuclear repulsion are obtained by the density functional-based tight-binding method [16]. This approach has been tested in detail for reaction energies, geometries, rotational and proton transfer barriers for a large set of small organic molecules [17] and yields very good results for homonuclear systems, such as silicon and carbon, and hydrocarbon systems [18].

The one-electron states are calculated at each time step by solving the time-dependent Schrödinger equation in a non-orthogonal basis:

$$i\hbar \frac{\partial \mathbf{\Psi}_j}{\partial t} = \mathbf{S}^{-1} \cdot \mathbf{H} \cdot \mathbf{\Psi}_j, \quad (3)$$

where $\mathbf{S}$ is the overlap matrix for the atomic orbitals. The laser pulse is characterised by the vector potential $\mathbf{A}$, which is coupled to the Hamiltonian through the time-dependent Peierls substitution [19]:

$$H_{ab}(\mathbf{X} - \mathbf{X}') = H_{ab}^0(\mathbf{X} - \mathbf{X}') \exp\left( \frac{iq}{\hbar c} \mathbf{A} \cdot (\mathbf{X} - \mathbf{X}') \right). \quad (4)$$

Here, $H_{ab}(\mathbf{X} - \mathbf{X}')$ is the Hamiltonian matrix element for the basis functions $a$ and $b$ on atoms at $\mathbf{X}$ and $\mathbf{X}'$, respectively, and $q = -e$ is the charge of the electron.

The nuclear motion is solved by the Ehrenfest equation of motion:

$$M_l \frac{\mathrm{d}^2 X_{l\alpha}}{\mathrm{d}t^2} = -\frac{1}{2} \sum_j \mathbf{\Psi}_j^+ \left( \frac{\partial \mathbf{H}}{\partial X_{l\alpha}} - i\hbar \frac{1}{2} \frac{\partial \mathbf{S}}{\partial X_{l\alpha}} \frac{\partial}{\partial t} \right) \mathbf{\Psi}_j - \partial U_{\text{rep}} / \partial X_{l\alpha}, \quad (5)$$

where $X_{l\alpha} = \langle \hat{X}_{l\alpha} \rangle$ is the expectation value of the time-dependent Heisenberg operator for the α-coordinate of the nucleus labelled by $l$ (with $\alpha = x, y, z$). Equation (5) is derived by neglecting the terms of the second and higher order in the quantum fluctuations $\hat{X} - \langle \hat{X}_{l\alpha} \rangle$ in the exact Ehrenfest theorem.

A unitary algorithm obtained from the equation for the time evolution operator [20] is used to solve the time-dependent Schrödinger equation (2). Equation (5) is numerically integrated with the velocity Verlet algorithm (which preserves phase space). A time step of 50 attoseconds was selected for this study. It was found that this time step produced energy conservation better than 1 part in $10^6$ in a 1 ps simulation.

The strengths of the present approach are that it retains all of the $3N$ nuclear degrees of freedom, and it includes both the excitation due to a laser pulse and the subsequent de-excitation at an avoided crossing near a conical intersection. The weakness of this method is that it amounts to averaging over all the terms in the Born–Oppenheimer expansion [21–25] rather than following the time evolution of a single term. However, when the process is dominated by many electron excitations, like the interaction of the $C_{60}$ fullerene with intense laser pulses, many electronically excited states are involved and the wave packet actually moves along a path weighted by all these electronic potential energy surfaces. In this case, the present approach yields very good results [26].

The initial geometry of the $C_{60}$ fullerene was simulated for 2000 fs relaxation at 298 K using the present technique prior to application of the laser pulse. The calculated lengths of the double bond and single bond are 1.397 and 1.449 Å, respectively, in close agreement with the experimental values [27]. The calculated HOMO–LUMO gap is 1.81 eV, which is in good agreement with the experimental value of 1.9 eV [28]. The ordering and degeneracy of the molecular orbital energy levels within 10 eV of the HOMO level are also in good agreement with experimental measurements [28]. A Gaussian shape laser pulse of 40 fs (FWHM) with a photon energy of 2.0 eV was chosen for this study. The $C_{60}$ fullerene was simulated for an additional 1000 fs without the laser pulse to generate the initial geometries for the dynamics simulation. From this trajectory, five geometries taken at equal time intervals were selected as starting geometries. Each trajectory was propagated for 4000 fs from the application of the laser pulse. In this paper, we focus on the response of $C_{60}$ to three different laser intensities: $0.44 \times 10^{12}$, $2.55 \times 10^{12}$ and $2.96 \times 10^{12}$ W/cm$^2$, which are denoted as intensity A, B and C, respectively, in the following discussion. For each of the laser intensities, the five trajectories yield very similar results and only one representative trajectory will be presented and discussed. The criterion for bond breaking is that the distance between two related carbon atoms becomes greater than 1.9 Å and no recombination of these two atoms is found in later simulation. The fragmentation criterion is that the distance between any two carbon atoms of two different fragments is greater than 1.9 Å and no bond formation is found between any two atoms in later simulation.

## 3. Results and discussion

Four snapshots taken from the simulation with the laser intensity B at various times are shown in Figure 1. Starting from the equilibrium geometry in the electronic ground state at 0 fs, the $C_{60}$ fullerene is electronically excited by the laser pulse. At about 200 fs (120 fs after laser irradiation), a greater number of C—C bonds have broken and the $C_{60}$ cage has been torn open. At about 800 fs, a $C_2$ dimer is observed to leave from the $C_{60}$ cage. After that, until the end of 2000 fs, no further bond cleavage has been observed. For the simulation with the laser intensity A, no C—C bond is found to be broken and the cage just takes vibrational motion during the simulation course. The trajectory with the laser intensity C shows a similar behaviour regarding the cage opening and fragmentation to the simulation with the laser intensity B.

Kinetic energy variations of $C_{60}$ with time for three trajectories resulted from three different laser intensities are presented in Figure 2. The number of C—C bonds broken at different times is also plotted in Figure 2 for comparison and discussion. For the laser intensity A (Figure 2(a)), by the end of laser irradiation, kinetic energy has risen up to about 1.2 eV because of the laser excitation of nuclear motion. This energy increases slightly after laser irradiation as a result of energy conversion. On the other hand, for the laser intensity C (Figure 2(c)), kinetic energy reaches to 6.0 eV at the end of the laser irradiation. Most impressively, kinetic energy has a quick increase after 80 fs, which is the duration of the laser pulse, and comes as high as 19.8 eV at 140 fs. The added kinetic energy after 80 fs comes from electronic energy through internal energy conversion, which is discussed in the following section. The increase in kinetic energy after the

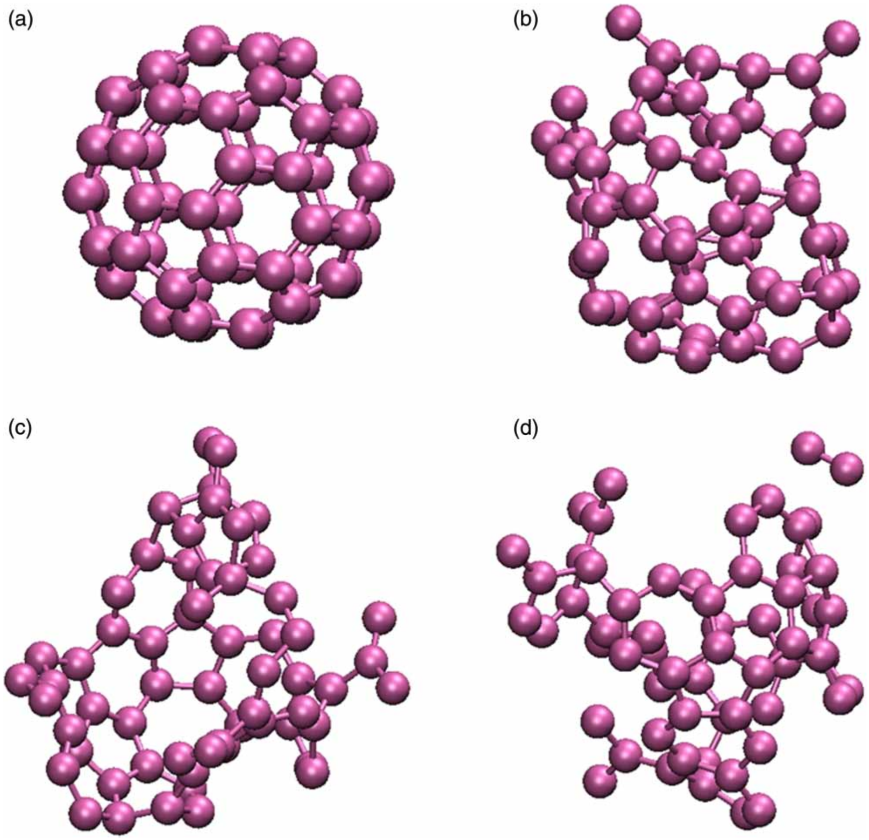

Figure 1. Snapshots taken at (a) 0, (b) 200, (c) 460 and (d) 808 fs for the simulation of $C_{60}$ fullerene response to a laser pulse of 40 fs (FWHM) with a photon energy of 2.0 eV and intensity of $2.55 \times 10^{12}$ W/cm$^2$.

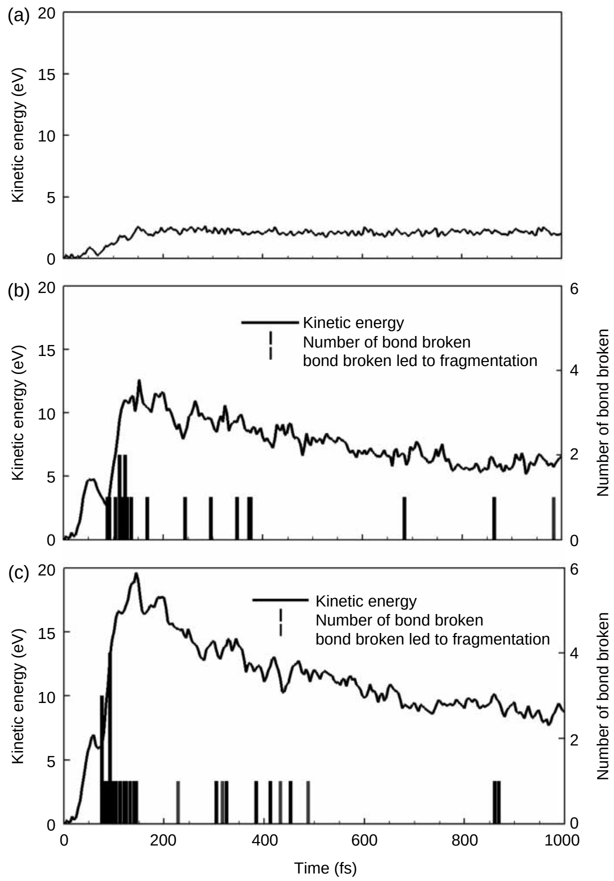

Figure 2. Time variations of the kinetic energy of $C_{60}$ fullerene subjected to the irradiation of a laser pulse of 40 fs (FWHM) with a photon energy of 2.0 eV and an intensity of (a) $0.44 \times 10^{12}$, (b) $2.55 \times 10^{12}$ and (c) $2.96 \times 10^{12}$ W/cm$^2$. The number of C—C bonds broken is also displayed in (b) and (c). Note that the grey bars show the number of bonds broken that leads to the formation of fragments.

laser irradiation is closely related to the breaking of the multiple C—C bonds, which leads to the opening of the $C_{60}$ cage but does not generate any fragmentation. Since the most significant bond dissociation is ahead of the maximum of kinetic energy in time, we, therefore, infer that the bond cleavage from 80 to 140 fs is a course rather than a result of kinetic energy increase. After 140 fs, kinetic energy starts to decrease and the rate of C—C bond breakage slows down. Dissociation of the C—C bonds at the times indicated by green bars in Figure 2(c) leads to the formation of fragments. Comparison of Figure 2(c) with (a), where no C—C bond breaking and no kinetic energy decrease are observed after 150 fs, indicates that the decrease in the kinetic energy of the $C_{60}$ for the laser intensity C is caused by the C—C bond breaking. The energy lost is converted to potential energy, which is discussed more in the following section. For the laser intensity B, as presented in Figure 2(b), the trajectory shows a similar relation between the kinetic energy variations and C—C bond breakage to the one observed for the trajectory with the laser intensity C.

Time variations of the electronic energy of $C_{60}$ for three trajectories resulted from three different laser intensities are presented in Figure 3. Compared with kinetic energy, the electronic energy gains a big increase due to the laser irradiation in each case, because of the excitation of multiple electrons from occupied molecular orbitals to unoccupied molecular orbitals [29]. Starting from −2922 eV, it increases to −2854 eV for laser intensity A, to −2589 eV for B and to −2536 eV for C. For laser intensity A, the electronic energy oscillates about its average value after the laser pulse duration. However, for both laser intensities B and C, the electronic energy shows a noticeable decrease from 90 fs to about 140 fs and a fluctuation about a constant value thereafter. The decrease in the electronic energy concurs with the increase in the kinetic energy in both cases, indicating that the partial electronic energy converts into the kinetic energy generated by C—C bond breakage during this period of time. In addition, as discussed in the following section, this process also leads to the conversion of a small fraction of electronic energy to potential energy.

Variations with time of potential energies of $C_{60}$ subjected to laser irradiation are plotted in Figure 4 for three different laser intensities. In each case, the potential energy shows a consequential drop after laser irradiation. From an initial value of 106 eV, it becomes 85 eV for the laser intensity A, 42 eV for B and 40 eV for C. After the application of the laser pulse, the potential energy for the laser intensity A varies around a constant value. The regular oscillation feature of the potential energy variations is associated with the breathing vibration of

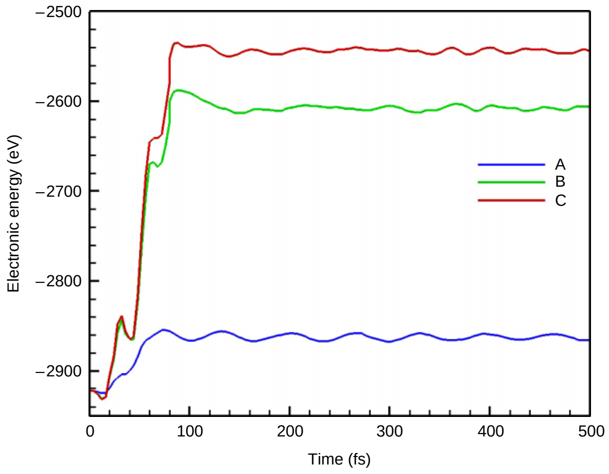

Figure 3. Time variations of electronic energy of $C_{60}$ fullerene under the irradiation of a laser pulse of 40 fs (FWHM) with a photon energy of 2.0 eV and an intensity of $0.44 \times 10^{12}$ (A), $2.55 \times 10^{12}$ (B) and $2.96 \times 10^{12}$ W/cm$^2$ (C).

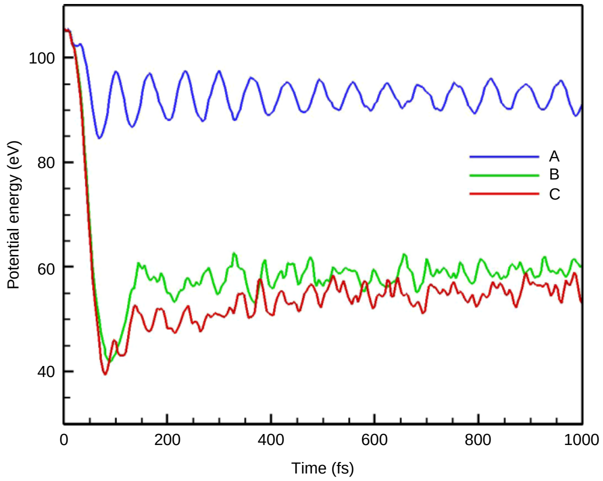

Figure 4. Time variations of the potential energy of $C_{60}$ fullerene under the irradiation of a laser pulse of 40 fs (FWHM) with a photon energy of 2.0 eV and an intensity of $0.44 \times 10^{12}$ (A), $2.55 \times 10^{12}$ (B) and $2.96 \times 10^{12}$ W/cm$^2$ (C).

the $C_{60}$ cage. On the other hand, soon after the end of the laser pulse, the potential energy for each of the laser intensities B and C starts to increase in a rate that is more pronounced before 140 fs. The quick increase in the potential energy before 140 fs results from the opening of the $C_{60}$ cage and the energy gained comes from the electronic energy through internal energy conversation. A slow increase in the potential energy after 140 fs for each of two laser intensities is also associated with C—C bond breaking but the energy gained comes from the kinetic energy. This is supported by the fact that the increases in the potential energies are accompanied by the decreases in the kinetic energies for this period of time, as shown in Figures 2 and 3.

By examining the variations of electronic, potential and kinetic energies, and comparing these variations with the features of C—C bond breakage, we arrive at the following conclusions. The $C_{60}$ cage opening induced by ultrafast laser pulse irradiation is an ultrafast non-thermal process. This ultrafast process provides a decay channel for photon-excited $C_{60}$ fullerene and converts partial electronic energy to kinetic energy and potential energy. Consequently, the $C_{60}$ fullerene gets very hot because of a quick increase in kinetic energy. The hot and damaged $C_{60}$ may take thermal fragmentation or non-thermal fragmentation. To explain the production of the hot $C_{60}$ cage, Laarmann and co-workers proposed the following mechanism: a strong, shaped laser pulse triggers a multielectron excitation via the $t_{1g}$ doorway state and the electronic excitation is followed by an efficient coupling to the symmetric breathing mode of the nuclear backbone of $C_{60}$ [30]. The simulation results presented above suggest an alternative heating mechanism. The bond breaking at the later process leads to the conversion of the kinetic energy into potential energy and eventually cools down the hot $C_{60}$ cluster. This process may or may not lead to fragmentation, as shown in Figure 2.

## 4. Conclusions

We have performed a semiclassical dynamics simulation study for the response of the $C_{60}$ fullerene to ultrashort laser pulse. The simulation results are summarised below.

(1) Irradiation with an ultrashort laser pulse deposits energy into the $C_{60}$ cage mainly through the excitation of multielectrons from the occupied molecular orbitals to unoccupied molecular orbitals. The increase in the potential energy and kinetic energy after the irradiation is relatively small.
(2) Irradiation with a strong ultrashort laser pulse leads to C—C bond breaking and fragmentation. However, sudden breaking of many C—C bonds in the early process leads to the opening of the $C_{60}$ cage, but does not generates any fragments. This is an ultrafast non-thermal process where a small fraction of the electronic energy is converted into the kinetic energy and potential energy. Consequently, $C_{60}$ is effectively heated up.
(3) C—C bond breaking after the ultrafast non-thermal process has the character of a thermal process, which leads to the conversion of kinetic energy into potential energy. Breakage of C—C bonds after the ultrafast non-thermal process may or may not generate fragments.

Some interesting questions concerning this simulation study are: (1) what is the threshold of laser intensity for $C_{60}$ cage opening, (2) is the ultrafast non-thermal process described above still a dominated one, if laser pulse intensity is just above the threshold and (3) how does the $C_{60}$ cage respond if laser intensity is much higher? Studies are under way to address these questions.

## Acknowledgements

This work is supported by the National Natural Science Foundation of China (No. 20773168). Acknowledgement is also made to the donors of the American Chemical Society Petroleum Research Fund for supporting this research at Nicholls State University. The Supercomputer Facility at Texas A&M University provided computational assistance.

## References

[1] E.E.B. Campbell, G. Ulmer, and I.V. Hertel, *Delayed ionization of $C_{60}$ and $C_{70}$*, Phys. Rev. Lett. 67 (1991), pp. 1986–1988.
[2] K.R. Lykke and P. Wurz, *Direct detection of neutral products from photodissociated $C_{60}$*, J. Phys. Chem. 96 (1992), pp. 3191–3193.
[3] I.V. Shchatsinin, T. Laarmann, G. Stibenz, G. Steinmeyer, A. Stalmoshonak, N. Zhavoronkov, C.P. Schulz, and I.V. Hertel, *$C_{60}$ in intense short pulse laser fields down to 9 fs: Excitation on time*

*scales below e–e and e–phonon coupling*, J. Chem. Phys. 125 (2006), pp. 194320/1–15.

[4] C. Lifshitz, *Ionization potentials and dissociation energies of neutral, singly and doubly charged C-n fullerenes from n=20 to 70*, Int. J. Mass Spectrom. 200 (2000), pp. 423–442.

[5] S.C. Brien, J.R. Heath, R.F. Curl, and R.E. Smalley, *Photophysics of buckminsterfullerene and other carbon cluster ions*, J. Chem. Phys. 88 (1988), pp. 220–230.

[6] C. Xu and G.E. Scuseria, *Tight-binding molecular dynamics simulations of fullerene annealing and fragmentation*, Phys. Rev. Lett. 72 (1994), pp. 669–672.

[7] E.E.B. Campbell, K. Hansen, K. Hoffmann, G. Korn, M. Tchaplyguine, M. Wittmann, and I.V. Hertel, *From above threshold ionization to statistical electron emission: The laser pulse duration dependence of $C_{60}$ photoelectron spectra*, Phys. Rev. Lett. 84 (2000), pp. 2128–2131.

[8] L. Horvath and T.A. Beu, *Tight-binding molecular dynamics simulations of radiation-induced fragmentation of $C_{60}$*, Phys. Rev. B 77 (2008), 075102/1–8.

[9] T.A. Beu and L. Horvath, *Tight-binding molecular dynamics simulations of radiation-induced $C_{60}$ fragmentation*, Phys. Rev. B 79 (2009), 054112/1–5.

[10] V.R. Bhardwaj, P.B. Corkum, and D.M. Rayner, *Internal laser-induced. Dipole force at work in $C_{60}$ molecule*, Phys. Rev. Lett. 91 (2003), 203004/1–4.

[11] M. Boyle, M. Hedén, C.P. Schulz, E.E.B. Campbell, and I.V. Hertel, *Two-color pump-probe study and internal energy dependence of Rydberg state excitation in $C_{60}$*, Phys. Rev. A 70 (2004), 051201/1–4.

[12] M. Boyle, T. Laarmann, K. Hoffmann, M. Hedén, E.E.B. Campbell, C.P. Schulz, and I.V. Hertel, *Excitation dynamics of Rydberg states in $C_{60}$*, Eur. Phys. J. D 36 (2005), pp. 339–351.

[13] H.O. Jeschke, M.E. Garcia, and J.A. Alonso, *Nonthermal fragmentation of C60*, Chem. Phys. Lett. 352 (2002), pp. 154–162.

[14] Y. Dou, B.R. Torralva, and R.E. Allen, *Semiclassical electron-radiation-ion dynamics (SERID) and cis–trans photoisomerization of butadiene*, J. Mod. Opt. 50 (2003), pp. 2615–2643.

[15] Y. Dou, B.R. Torralva, and R.E. Allen, *Interplay of electronic and nuclear degrees of freedom in a femtosecond-scale photochemical reaction*, Chem. Phys. Lett. 392 (2004), pp. 352–357.

[16] M. Elstner, D. Porezag, G. Jungnickel, J. Elsner, M. Haugk, T. Frauenheim, S. Suhai, and G. Seifert, *Self-consistent-charge density-functional tight-binding method for simulations of complex materials properties*, Phys. Rev. B 58 (1998), pp. 7260–7268.

[17] M. Elstner Dissertation, University of Paderborn, Germany Elstner, 1998.

[18] T. Frauenheim, G. Seifert, M. Elstner, T. Niehaus, C. Kohler, M. Armkreutz, M. Sternberg, Z. Hajnal, A. diCarlo, and S. Suhai, *Atomistic simulations of complex materials: Ground and excited state properties*, J. Phys.; Condens. Matter. 14 (2002), pp. 3015–3047.

[19] M. Graf and P. Vogl, *Electromagnetic fields and dielectric response in empirical tight-binding theory*, Phys. Rev. B 51 (1995), pp. 4940–4949.

[20] R.E. Allen, T. Dumitrica, and B.R. Torralva, *Ultrafast Physical Processes in Semiconductors*, K.T. Tsen, ed., Academic, New York, 2001.

[21] M. Born and J.R. Oppenheimer, *Zur Quantentheorie der Molekeln*, Ann. Phys. (Leipzig) 84 (1927), pp. 457–477.

[22] E. Teller, *The crossing of potential surfaces*, J. Phys. Chem. 41 (1937), p. 109.

[23] M. Born and K. Huang, *The Dynamical Theory of Crystal Lattices*, Oxford University Press, London, 1954.

[24] W. Domcke, D.R. Yarkony, and H. Köppel, *Conical Intersections: Electronic Structure, Dynamics, and Spectroscopy*, World Scientific, Singapore, 2004.

[25] M. Baer, *Beyond Born–Oppenheimer: Electronic Nonadiabatic Coupling Terms and Conical Intersections*, Wiley, Hoboken, NJ, 2006.

[26] B.R. Torralva, T.A. Niehaus, M. Elstner, S. Suhai, T. Frauenheim, and R.E. Allen, *Response of $C_{60}$ and $C_n$ to ultrashort laser pulses*, Phys. Rev. B 64 (2001), 153105/1–4.

[27] C.S. Yannoni, P.P. Bernier, D.S. Bethune, G. Meijer, and J.R. Salem, *An NMR determination of the bond lengths in C60*, J. Am. Chem. Soc. 113 (1991), pp. 3190–3192.

[28] D.R. McKenzie, C.A. Davis, D.J.H. Cockayne, D.A. Muller, and A.M. Vassallo, *The structure of the C70 molecule*, Nature 355 (1992), pp. 622–624.

[29] H.J. Li, H. Tang, and Y. Dou, *Laser induced nonthermal fragmentation of $C_{60}$ studied by semiclassical dynamics simulation*, Mol. Phys. 107 (2009), pp. 2039–2044.

[30] T. Laarmann, I. Shchatsinin, A. Stalmashonak, M. Boyle, N. Zhavoronkov, J. Handt, R. Schmidt, C.P. Schulz, and I.V. Hertel, *Control of giant breathing motion in $C_{60}$ with temporally shaped laser pulses*, Phys. Rev. Lett. 98 (2007), 058302/1–4.